

Prospective Subsurface Hydrocarbon Accumulations and Their Association with Source and Reservoir Rocks Using Airborne Spectral Gamma-Ray Data, West Aswan, Egypt

Ali Mohamed Mostafa Mohamed*

Exploration Division, Nuclear Materials Authority, P.O. Box: 530, Maadi, Cairo, Egypt.

Received: 25 Dec. 2025, Revised: 15 Feb. 2026, Accepted: 1 Mar. 2026

Published online: 1 May. 2026

Abstract: Besides employing aerial spectral gamma-ray data for geological mapping, radioactive deposit exploration, and radiation dose evaluation, additional uses encompass thorium normalization to ascertain the possible existence of subsurface hydrocarbon resources. Recently, measures of radiogenic heat production (RHP) have been employed to distinguish between reservoir and source rocks of hydrocarbons in the west Aswan area, southwestern desert, Egypt. The histogram technique was applied to illustrate the distribution of calculated radiogenic heat production values in the study area. It was found that about 50.4 percent of values are more than $1.64 \mu\text{W}/\text{m}^3$, which was calculated as the arithmetic mean of the RHP value. The statistical analysis of RHP values, which was calculated among the different rock units in the study area, illustrates that the standard deviation value was calculated as $0.5 \mu\text{W}/\text{m}^3$, and the values ranged from $0.03 \mu\text{W}/\text{m}^3$ as a minimum to a maximum value of $3.72 \mu\text{W}/\text{m}^3$. Values exceeding $1.64 \mu\text{W}/\text{m}^3$ signify the existence of hydrocarbons linked to the rocks exhibiting these values. These rocks can be categorized as reservoir rocks, characterized by radiogenic heat production values between the arithmetic mean of $1.64 \mu\text{W}/\text{m}^3$ and the arithmetic mean plus one standard deviation, as $2.14 \mu\text{W}/\text{m}^3$. Rocks with radiogenic heat production rates exceeding $2.14 \mu\text{W}/\text{m}^3$ are designated as source rocks for hydrocarbons. Farafra formations constitute the fundamental units of the Thebes Group, deposited during the Eocene age. It is linked to the reservoir rocks in the research area, as corroborated by its lithological composition. The Farafra Formation consists of alveolinid white to grey limestone deposits, whereas the Dakhla Formation, deposited during the late Cretaceous age, is composed of submarine fan deposits of yellowish carbonate-bound siltstone and sandstone intercalated with clay, which increases the possibility of them being hydrocarbon source rocks.

Keywords: Radiogenic Heat Production, West Aswan, Farafra Formation, Ariel Gamma-ray Spectrometric Data.

1 Introduction

The investigating area is located in the southern region of the Egyptian Western Desert. The area encompasses approximately 11500 km^2 , situated between latitudes $24^\circ 10' \text{ N}$ and $25^\circ 25' \text{ N}$, and longitudes $31^\circ 07' \text{ E}$ and $32^\circ 05' \text{ E}$. Sedimentary rocks predominantly encompass the study area.

Since the early 1950s, petroleum explorationists have employed gamma-radiation measurements as a strategy for hydrocarbon prospecting [1]. The rate of radiogenic heat production (RHP) in crustal rocks is primarily influenced by three radioactive elements: uranium (U), thorium (Th), and potassium (K). These possess extensive half-lives akin to the Earth's age (see Table 1). In radioactive decay, mass is transformed into energy.

The energy from released particles and gamma radiation linked to various decay processes is absorbed by rocks and ultimately converted into heat. Around 45% of the surface heat flow detected over continents originated from radionuclides within the crust. In contrast, the intensity of surface heat flow diminishes exponentially with depth. Measurements of RHP indicate that acidic rocks have the highest production rate, followed by basic and then ultrabasic rocks [2].

The overall heat generation rate (A) of rocks is the aggregate of the individual contributions from uranium, thorium, and potassium (A_U , A_{Th} , A_K), respectively [2]. [3] Use the areal gamma ray spectrometric data to map the radiogenic heat production of the Gabal Duwi area of Egypt.

*Corresponding author e-mail: Ali_ellaban2006@yahoo.com

The statistical analysis method for the radioactive heat values produced by the three radioactive elements (K, eU, and eTh) was initially employed by [4], specifically applied to clastic sedimentary rocks. In 2025, [5] employed this approach on carbonate rocks, achieving superior findings relative to various well log investigations.

[6] Documented the potential for hydrocarbon deposition in Thebes's group rock units by employing a thorium normalization technique with aerial gamma ray spectrometric data in the Abu-Zeneima El-Tour region of southwestern Sinai, Egypt.

Geological Setting

The study area includes a distinctive array of geomorphological characteristics, such as the Nile River, Nubian Plain, Wadi Kurkur, Kurkur Oasis, playa, isolated hills, and Sinn El-Kaddab plateau (Figure 1).

Sinn El-Kaddab plateau, encompassing the study area, is intersected by several faults, predominantly oriented east-west, with additional orientations of north-south and southwest-northeast (Figure 2). The faults possess strike lengths ranging from several kilometers to in excess of 100 kilometers.

A substantial Phanerozoic sequence in the Kurkur area (Figure 3) constitutes the Sinn El-Kaddab plateau (about 497 meters above sea level). The succession is unconformably superimposed on the Neoproterozoic basement rocks (pink granite). It commences with Cretaceous continental Nubia Sandstone and is capped by Quaternary travertine, consisting of silicified carbonate from terrestrial hot springs.

The stratigraphic sequence has been well documented by [7 & 8], and many later workers (e.g., [9] to name some):

**** Farafra Formation** (Late Eocene) consists of alveolinid white to grey limestone deposits,

**** Dungul Formation** (Early to Middle Eocene) constitutes the cap rock of the Sinn El-Kaddab plateau. The Dungul Formation comprises alternating strata of shale and limestone, with thicknesses varying from 40 to 127 meters.

**** Garra Formation** (Late Paleocene to Early Eocene) consists of substantial (60-127 m) limestones interspersed with chalk, marl, and shales, formed in shallow maritime shelves to deeper marine paleoenvironments.

**** Kurkur Formation** (Early Paleocene) consists of two

siliceous limestone layers interspersed with clastic sediments and sporadic localized phosphate components. The local limestones include numerous marine invertebrate fossils. The Kurkur Formation's sediments were deposited in shallow marine conditions during the early Paleocene epoch.

****Dakhla Formation** (Cretaceous eMaastrichtian) is a marine sequence consisting of interbedded shales, sandstones, and conglomerates at the base, with carbonate beds creating a ledge at the top. The Dakhla Formation varies in thickness from 39 to 250 meters and diminishes towards the west. Near Kurkur Oasis, some marine fossil shells and rip-up clasts are evident. The Dakhla Formation is situated conformably above the Nubia Formation.

**** Nubia Formation** (pre-Cretaceous) consists of well-sorted, loosely cemented 2 mm quartz sandstone characterized by tabular cross-bedding and asymmetric ripple lines. The Nubia Formation exhibits a thickness ranging from around 400 to 600 meters, with a maximum recorded thickness of 592 meters in the Kurkur Oasis region [8]. The fluctuating thickness of the Nubian, along with shallow dip angles, implies that the Precambrian Basement possesses an uneven surface, signifying a disconformity [10].

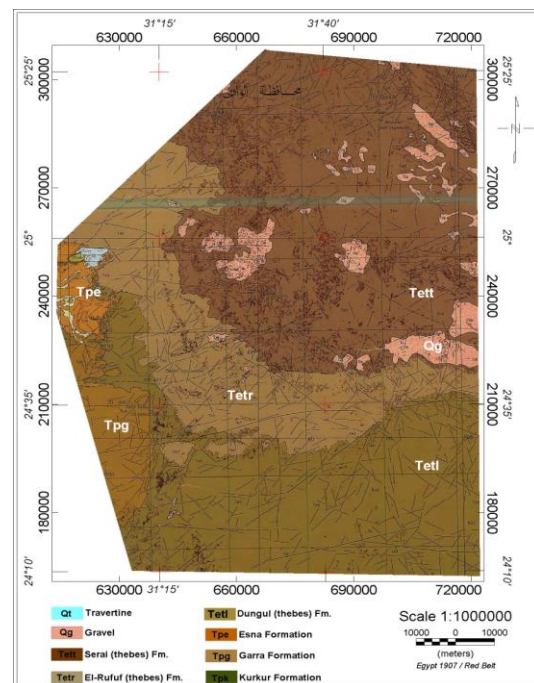


Fig.1: Geological map of the study area.

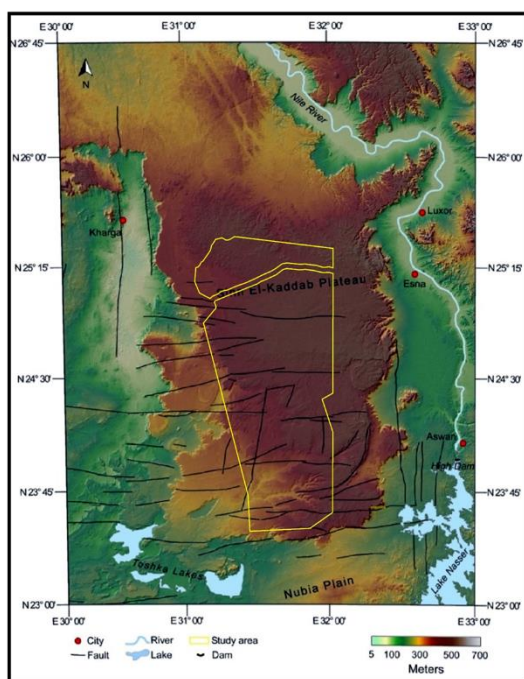


Fig.2: The topographic and structural map of the Sinn El-Kaddab Plateau.

Airborne Spectral Gamma-Ray Data

The airborne spectral gamma-ray scan was executed along parallel flight lines directed northwest-southeast, perpendicular to the dominant geological strike, with a separation of one kilometer. Spectral radiometric data were

obtained with a sampling interval of 70 m (230 feet) at a nominal sensor altitude of 120 m (terrain clearance). The survey was executed by a twin-engine Beechcraft King Air B200SE aircraft. This aircraft can operate within a speed range of 222 km/h to 250 km/h.

A very sensitive 256-channel airborne gamma-ray spectrometer equipped with a primary 50.3-liter thallium-activated sodium iodide detector was utilized. For additional information regarding the survey equipment utilized and flight operations, please consult the final operation report. [11] provides a discussion on airborne radiometric surveying procedures, encompassing instrumentation, reporting methods, system calibration, and gamma-ray energy windows.

Figures 4 to 6 show color maps of the apparent surface concentrations of radioelements [potassium (K) in %, equivalent uranium (eU) and thorium (eTh) in ppm, respectively]. This can be seen in the good correlation between the radioactive maps and the mapped geology (Figure 2). Separate radio-element maps are also useful to identify certain rock types.

Figure 4 shows that potassium concentrations range from 0.01 % to 1.93%. The highest concentrations were recorded in the northeastern part of the region, associated with the Eocene-era Thebes rocks. Also, Thebes's group rocks have the highest concentrations of eU and eTh as illustrated in figures 5 & 6. The highest concentrations of both equivalent uranium and equivalent thorium reach 17 and 23 ppm, respectively.

Age	Rock Units		Lithology	Environments & Facies
Quaternary	Q. travertine		Silicified carbonate	Terrestrial hot springs
Eocene Ypresian	Dungul Formation	Naqb Dungul Limestone Member	Reefal limestones Shelly Limestones Marly Limestones	Shallow ramp Shoal reef Hemi-pelagic
		Abu Ghurra Shale Member	Shale and silty shale	Open marine
Paleocene Thanetian	Garra Formation		Shelly limestones Benthic foraminiferal limestones Shale	Shallow marine Lagoon Delta
	Kurkur Formation		Brown reefal and shelly limestones, very hard compact.	Littoral marine
Late Cretaceous Maastrichtian	Dakhla Formation		Pale green to grey foraminiferal shale, sandy clay, fine grained sandstone, gypsiferous.	Open marine
Cretaceous	Nubia Sandstone		Sandstones, siltstones and claystones	Continental with marine embayments
Pre-Cambrian	Basement Rocks		Pink granites	

Fig. 3: Tentative stratigraphic composite section of the Kurkur area. After [8 & 9].

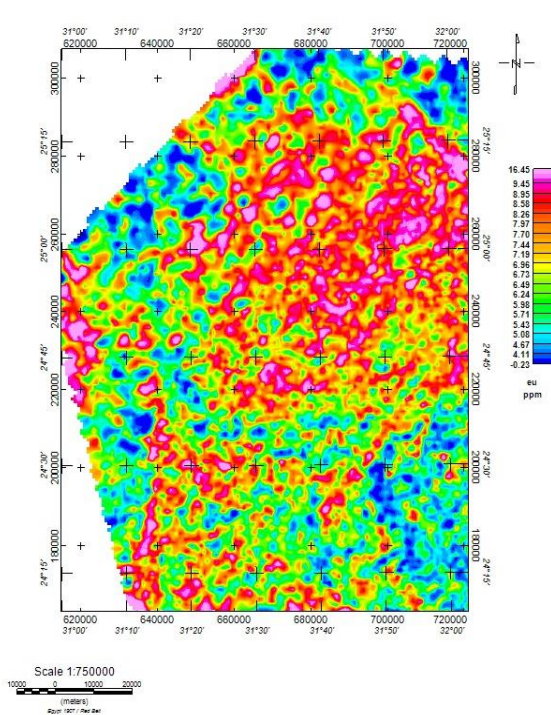
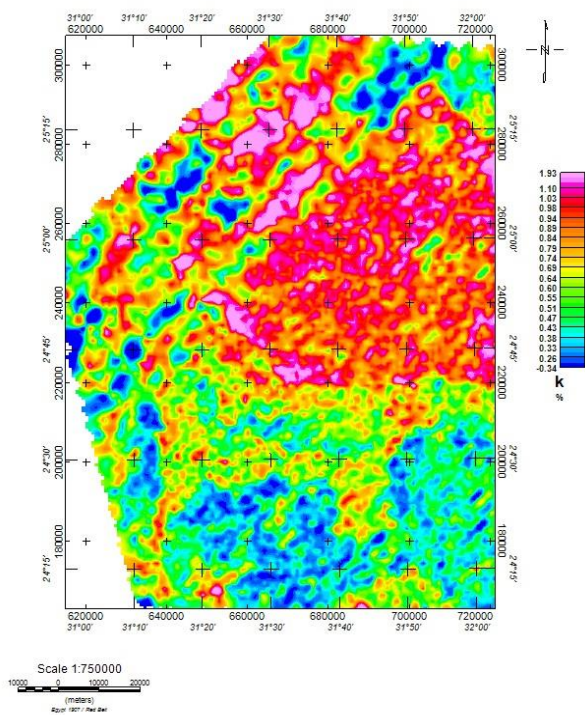


Fig. 4: Potassium color map of West Aswan area, South Western Desert, Egypt.

Fig. 5: Equivalent Uranium color map of the West Aswan area, South Western Desert, Egypt.

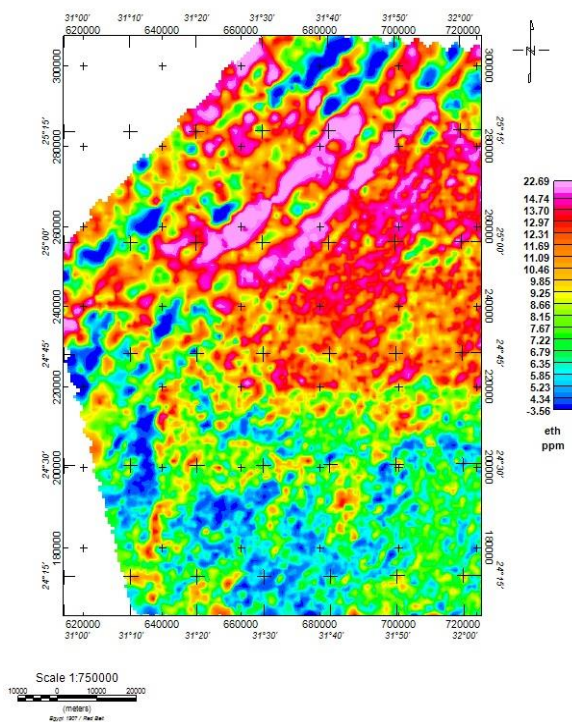


Fig. 6: Equivalent Thorium color map of West Aswan area, South Western Desert, Egypt.

2 Methodology

Radiogenic Heat Production (RHP):

If a rock's density (ρ) and its concentrations in uranium (CU), thorium (CTh), and potassium (CK) are known, its radiogenic heat generation rate (A) can be determined. Using any of the values for eU, e Th, and K, the formula by [2] yields:

$$A (\mu\text{Wm}^{-3}) = \rho (0.0925\text{Cu} + 0.0256\text{Cth} + 0.0348\text{Ck})$$

Where ρ represents the dry density of rock (g/cm^3) and CU, CTh, and CK denote the concentrations of U and Th in ppm and K in %, respectively. Rybach's formula requires prior knowledge about the density and concentration of the radioelements U, Th, and K within the rock. Radioactive heat generation has been determined from laboratory measurements of radio-element concentrations [12] and directly from gamma-ray logs [13]. Radioactive heat generation has also been approximated using airborne gamma-ray data [14 & 15].

Calculated the average density for each rock unit (Table 1) based on the densities provided by [16]. Determining a statistical average density estimate for each rock unit proved to be somewhat challenging. Some geological units comprise various rock types, such as sedimentary, metasedimentary, and metavolcanic. The density values for basement samples varied from 2.59 g/cm^3 for granites to 2.92 g/cm^3 for more mafic diorites and gabbros. The densities of sedimentary rocks varied from 2.00 g/cm^3 for sandstone to 2.62 g/cm^3 for silicified limestone.

Table (1): Average density for each rock unit

Rock	Density g/cc
Sedimentary	2.41
Metasediments	2.62
Metavolcanics	2.64
Hammamat	2.61
Dokhan Volcanic	2.6
Granites	2.95

A novel technique developed by [4] to distinguish between saturated and hydrocarbon-free rocks, and to ascertain the correlation of saturated hydrocarbon zones with source or reservoir rocks by statistical analysis of RHP measurements. The reservoir rocks demonstrate RHP values consistent with the interval between the arithmetic mean and the arithmetic mean plus the standard deviation,

while the source rocks show RHP values surpassing the arithmetic mean plus the standard deviation.

3 Discussions

The estimated values of radioactive heat generation (Figure 7) are determined by the quantities of uranium, thorium, and potassium obtained from airborne surveys, and hence represent surface or apparent values. The production of radioactive heat significantly varies according to the type of rock. This elucidates the strong link between the radioactive heat generation map (Figure 7) and the geological mapping (Figure 1), where the highest radiogenic values were recorded associated with Thebes group rocks, which consist of Farafra Formations and the late Cretaceous age, which consists of Dakhla Formations.

From the statistical analysis of calculated radiogenic heat production values in the study of the West Aswan area, it can be noticed that the region exhibits a spectrum of radioactive heat generation from 0.03 $\mu\text{W/m}^3$ to 3.72 $\mu\text{W/m}^3$, with an average value 1.64 $\mu\text{W/m}^3$, and the standard deviation value was calculated as 0.49 $\mu\text{W/m}^3$.

The histogram (Figure 8) depicting the distribution of radiogenic heat production data indicates that values ranging from 1.2 to 2.4 $\mu\text{W/m}^3$ account for about 90% of the dataset. Values below 1.2 $\mu\text{W/m}^3$ account for around 3%, indicating that 7% of the data surpasses 2.4 $\mu\text{W/m}^3$.

According to the innovative technique applied by Nabih and Al-Alfy in 2021, Figure No. 8 illustrates that the blue zones, which exhibit values below the average radiogenic heat production (1.63 $\mu\text{W/m}^3$), signify rocks devoid of hydrocarbon materials.

The green zones have radiogenic heat production values between average and average plus standard deviation values (1.63 and 2.13 $\mu\text{W/m}^3$), correlating with the Farafra Formation rocks, composed of limestone, substantiating their potential classification as reservoir rocks.

Radiogenic heat production values exceeding the average plus standard deviation value 2.13 $\mu\text{W/m}^3$ are depicted in Figure 8 by red zones, indicating the geology of the Dakhla Formation, which consists of deposits of yellowish carbonate-bound siltstone and sandstone intercalated with clay, thereby affirming its hydrocarbon content and categorizing it as a source rock [17-21].

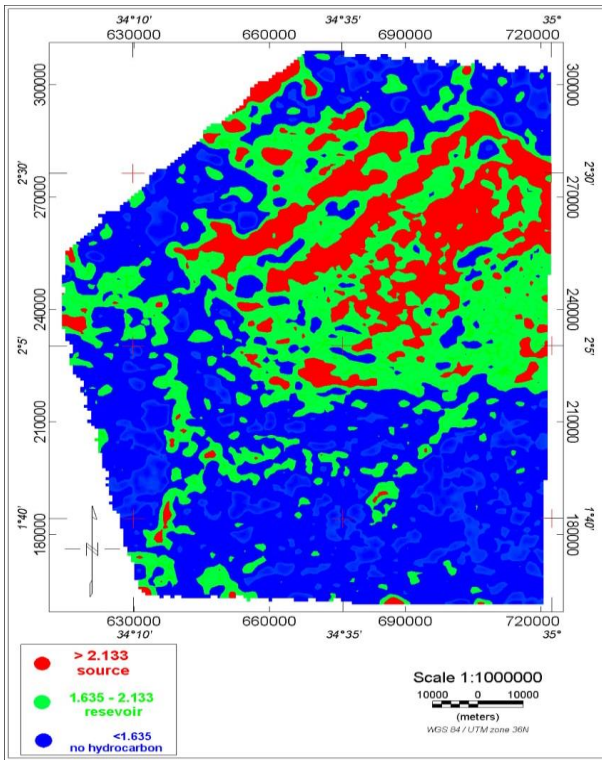


Fig. 7: Radiogenic Heat Production color map of the West Aswan area, South Western Desert, Egypt.

4 Conclusions

Thebes Group, deposited during the Eocene age, consists of the Serai Formation, which is composed of clay intrusions interspersed with brown limestone, and the Farafra Formation, which consists of alveolinid white to grey limestone deposits. The Dakhla formation, deposited during the late Cretaceous age, is composed of submarine fan deposits of yellowish carbonate-bound siltstone and sandstone intercalated with clay.

The statistical analysis of calculated radiogenic heat production values in the study area of West Aswan shows that the region exhibits a spectrum of radioactive heat generation from $0.03 \mu\text{W}/\text{m}^3$ to $3.72 \mu\text{W}/\text{m}^3$, with an average value of $1.64 \mu\text{W}/\text{m}^3$, and the standard deviation value was calculated as $0.49 \mu\text{W}/\text{m}^3$.

The distribution of radiogenic heat production data indicates that values ranging from 1.2 to $2.4 \mu\text{W}/\text{m}^3$ account for about 90% of the dataset. Values below $1.2 \mu\text{W}/\text{m}^3$ account for around 3%, indicating that 7% of the data surpasses $2.4 \mu\text{W}/\text{m}^3$.

According to the radiogenic heat production values of Farafra Formation rocks, which are composed of limestone, substantiating their potential classification as reservoir rocks. While the Dakhla Formation can be classified as a source rock.

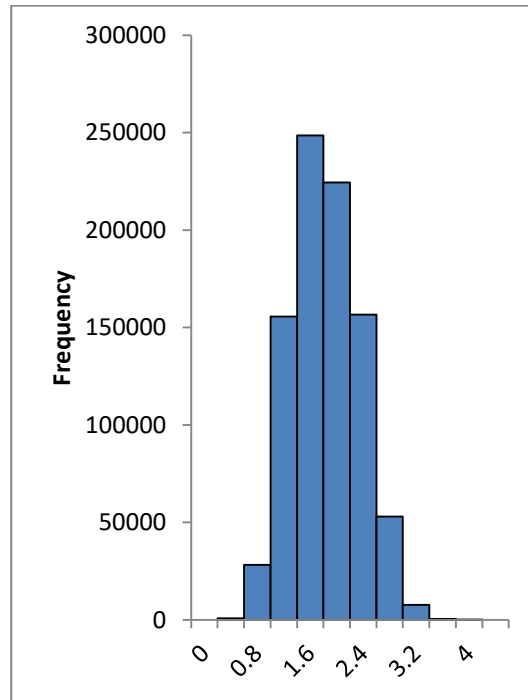


Fig. 8: Radiogenic Heat Production Histogram of the West Aswan area, South Western Desert, Egypt.

Acknowledgments

The assistance of Nuclear Materials Authority (NMA), for the provision of the area survey data, is gratefully acknowledged to Airborne Geophysics Department (AGD) and Prof. Ibrahim Al-Alfy for their help during the course of this work.

References

- [1] Armstrong, F.E., Heemstra, R.J., 1973: Radiation Haloes and Hydrocarbon Reservoirs: A Review. US Bureau of Mines Information Circular, pp. 52–79.
- [2] Rybach, L., 1988: Determination of heat production rate, in R. Hänel, L. Rybach, and L. Stegena, eds., Handbook of terrestrial heat flow density determination: Kluwer, 125–142.
- [3] Salem A., Elsirafy A., Aref A., Ismail A., Ehara S., and Ushijima K., 2005: Mapping Radioactive Heat Production from Airborne Spectral Gamma-Ray Data of Gebel Duwi Area, Egypt. Proceedings World Geothermal Congress, Antalya, Turkey, pp 1-6.
- [4] Nabih M., and Al-Alfy I. M., 2021: Differentiation between source and reservoir rocks using statistical analysis of radiogenic heat production: A case study on Alam El Bueib Formation, Northwestern Desert, Egypt, Applied Radiation and Isotopes 176, 2021, 109868

- [5] Al-Alfy I. M., Ghoneimi A., Kamel M. A., and Nabih M., 2025: Integrating thorium normalization and radiogenic heat production for distinguishing reservoir and source rocks in Abu Roash Formation, Western Desert, Egypt, Egyptian Petroleum Research Institute (EPRI). Pp. 22 – 31. <https://doi.org/10.62593/2090-2468.1060>
- [6] Shaheen M. A., Abd El Salam H. F., El Hawary A. M., 2022: Aerial gamma-ray spectro-metric data as a guide for probable hydrocarbon accumulations at Abu-Zeneima/Al-Tur area, Southwestern Sinai, Egypt. Appl. Radiat. Isot., 186, 110290. [doi: 10.1016/j.apradiso.2022.110290](https://doi.org/10.1016/j.apradiso.2022.110290).
- [7] Said, Rushdi, 1962: The Geology of Egypt. Elsevier Publishing Company, Amsterdam and New York.
- [8] Issawi, Bahay, 1968: The Geology of Kurkur and Dungul Area, Egyptian Geological Survey, Paper No. 46, 102.
- [9] Tantawy, A. A., 1994: Paleontological and Sedimentological Studies on the Late Cretaceous-Early Tertiary Succession at Wadi Abu Ghurra-Gabal El-Kaddab Stretch, South Western Desert, Egypt. M.Sc. Thesis, Aswan Faculty of Science, Asyut Univ.
- [10] Khamies, A.A. El-Tarras, M.M. and Haridy, H. M. M., 2004: Airborne gamma ray spectrometric and magnetic signatures in relation to geological structures and their implication on uranium distribution in the Northern Eastern Desert, Egypt, pp. 225-238.
- [11] International Atomic Energy Agency (IAEA), 1991: Airborne gamma-ray spectrometer survey. Technical Reports Series No. 323, Vienna, Austria, 97 p.
- [12] Fernández M., Marzan I., Correia A., and Ramalho E., 1998: Heat flow, heat production, and lithosphere thermal regime in the Iberian Peninsula, Tectonophysics 291, 29-53. <https://doi.org/10.1016/j.apradiso.2021.109868>
- [13] Bücker C. and Rybach L., 1996: A simple method to determine heat production from gamma-ray logs, Marine and Petroleum Geology 13, 373-375.
- [14] Richardson, K.A., and Killeen, P.G., 1980: Regional radiogenic heat production mapping by airborne gamma-ray spectrometry; in Current Research, Part B, Geological Survey of Canada, Paper 80-1B, p.227-232.
- [15] Thompson, P.H., Judge, A.S., Charbonneau, B.W., Carson, J.M., and Thomas, M.D., 1996: Thermal regimes and diamond stability in the Archean Slave Province, Northwestern Canadian Shield, District of Mackenzie, Northwest Territories; in Current Research, 96-1E, Geological Survey of Canada, P. 135-146.
- [16] Shaaban M.A., 1973: Geophysical studies on the lead Zinc mining district between Quseir and Mersa Alam, Red Sea coast, Eastern Desert, Egypt, Ph.D. thesis No 568, Cairo University, Cairo, Egypt.
- [17] Oraby, AH., Saleh, GM., Hassan, EM., Eldabour, SE., El Tohamy, AM., Kamar, MS., El Feky, MG., El Taher, A., (2022) Natural radioactivity and radioelement potentiality of mylonite rocks in Nugrus Area, Southeastern Desert, Egypt. Radiochemistry 64 (5), 645-655.
- [18] Abdel Gawad, AE., Ghoneim, MM., El-Taher, A., Ramadan, AA., (2021) Mineral chemistry aspects of U-, Th-, REE-, Cu-bearing minerals at El-Regeita shear zone, South Central Sinai, Egypt. Arabian Journal of Geosciences 14 (14), 1356.
- [19] El-Taher, A., Badawy, WM., Khater, AEM., Madkour, HA., (2019) Distribution patterns of natural radionuclides and rare earth elements in marine sediments from the Red Sea, Egypt. Applied Radiation and Isotopes 151, 171-181.
- [20] Mohamed M Ghoneim, Elena G Panova, Ahmed E Abdel Gawad, Hamdy A Awad, Hesham MH Zakaly, Atef El-Taher., (2023) Analytical methodology for geochemical features and radioactive elements for intrusive rocks in El Sela area, Eastern Desert, Egypt. International Journal of Environmental Analytical Chemistry 103 (6), 1272-1291.
- [21] Wael M Badawy, Andrey Yu Dmitriev, Hussein El Samman, Atef El-Taher, Maksim G Blokhin, Yasser S Rammah, Hashem A Madkour, Safwat Salama, Sergey Yu Budnitskiy., (2024) Elemental composition and metal pollution in Egyptian Red Sea mangrove sediments: characterization and origin. Marine Pollution Bulletin 198, 115830.